Biophysical Journal, Volume *111*

Supplemental Information

Nanosecond Dynamics of Gαi1 Bound to Nucleotides or Ric-8A, a Gα Chaperone with GEF Activity

Labe A. Black, Celestine J. Thomas, Gwendolyn N. Nix, Michelle C. Terwilliger, Stephen R. Sprang, and J. B. Alexander Ross

Nanosecond dynamics of the heterotrimeric G protein subunit Giα1 when bound to nucleotides or Ric-8A, a Gα chaperone with GEF activity

Supporting Material

L.A. Black[1,2,5], C.J. Thomas[1,2,6], G.N. Nix[1,3],
M.C. Terwilliger[1,2], S.R. Sprang[1,3,*], J.B.A. Ross[1,2,*]

[1]Center for Biomolecular Structure and Dynamics, [2]Department of Chemistry and Biochemistry, [3]Division of Biological Sciences, [4]Biochemistry Program, University of Montana, Missoula, MT, 59812; [5]current address, Rensselaer Polytechnic Institute, Troy, NY 12180; [6]current address, Regeneron Pharmaceuticals, Inc., Tarrytown, NY 10591.

*To whom correspondence may be addressed. Email: sandy.ross@umontana.edu or stephen.sprang@umontana.edu.

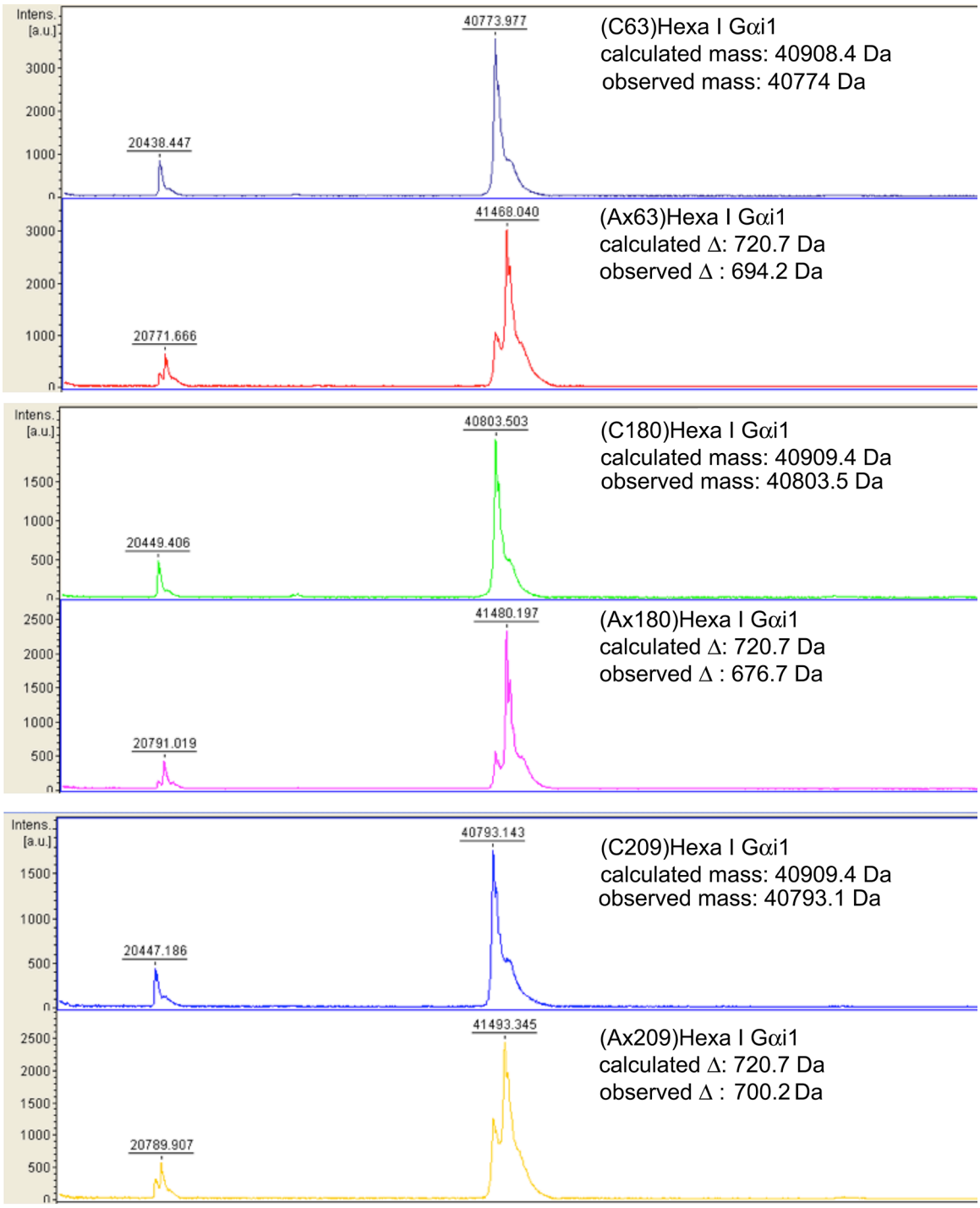

Figure S1 MALDI-ToF mass spectra of representative Gαi1 Hexa I Cysteine mutants (C63, C180 and C209) and their Alexa 488 (C5) adducts. "Δ" Values represent the observed or calculated mass difference between the Gαi1 Hexa I cysteine mutant and its Alexa 488(C5) adduct.

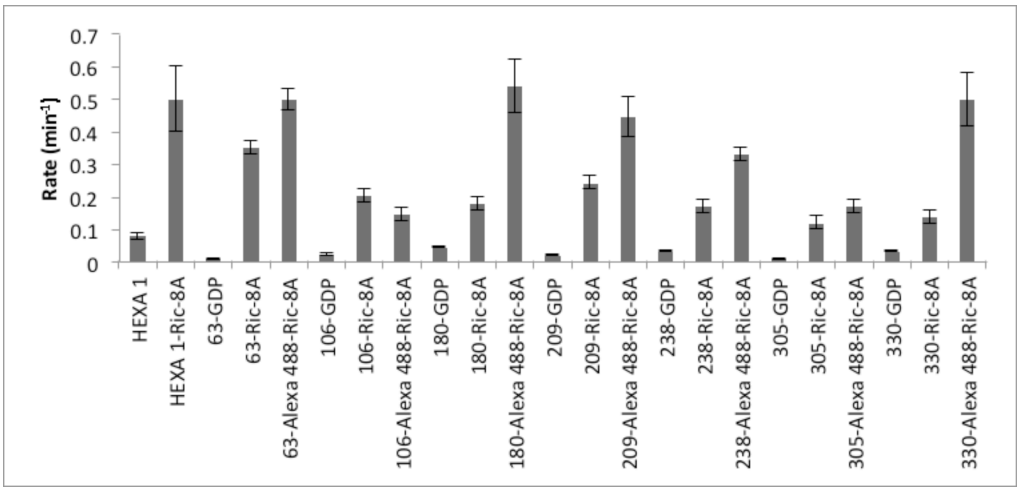

Figure S2 Intrinsic and Ric-8A-catalyzed GTPγS binding rates of Gαi1 Hexa I cysteine mutants and their Alexa 488(C5) adducts. GTPγS binding was assayed by the change in intrinsic tryptophan fluorescence as described (see main text). Briefly, freshly prepared Gαi1 (both labeled and unlabeled) were diluted to 1 μM in 20 mM HEPES pH 8.0, 100 mM NaCl, 10 mM Mg^{2+}, 0.05% C12E10 in the presence of absence of 1.5 μM Ric-8A. GTPγS was added to the sample at a final concentration of 10 μM to initiate nucleotide exchange. The reaction was monitored by emission at 340 nm after excitation at 295 nm (10-nm bandpass excitation and emission) continuously for 20 min using a Perkin-Elmer LS 55 luminescence fluorimeter. Three individual data sets for each sample were globally fit to a single exponential function to determine the rate using the program OriginPro 9.0.

TIME-RESOLVED FLUORESCENCE ANISOTROPY

Data collection: fluorescence anisotropy decay measurements were carried out using the FLASC 1000 (Quantum Northwest, Liberty Lake, WA), as described (1). Excitation was provided by ~ 70 ps pulses (FWHM) at a repetition rate of 10 MHz from a 470-nm laser diode (LDH-P-C-470; PicoQuant GmbH, Berlin). Vertical or horizontal components of excitation were selected by a rotating Glan-Thompson polarizer (Karl-Lambrecht, Chicago, IL). The vertical and horizontal components of the emission (VV and VH, respectively, with vertical excitation) were resolved by a beam-splitting Glan-Thompson polarizer (Karl-Lambrecht, Chicago, IL), thereby allowing simultaneous collection of of VV and VH decay curves. The fluorescence emission was selected by 525/50-nm (Chroma Technology Corp., Bellows Falls, VT) band-pass filters, and IBH model TBX-04 photomultipliers (Glasgow, Scotland) were used for single-photon counting. V and H decay curves were collected semi-simultaneously for equal times using a PRT 400 router and TimeHarp 200 PCI board (PicoQuant GmbH, Berlin) until $4x10^4$ counts (timing resolution of 35 ps/channel) were obtained at the maximum of the V curve. The instrument response function (IRF) is scatter from colloidal silica.

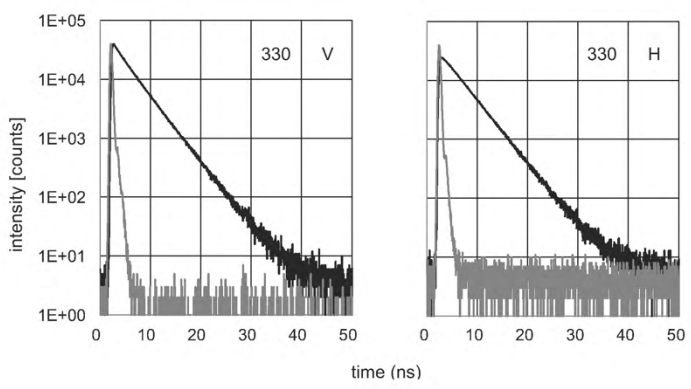

Figure S3 Anisotropy decay data: Ax330 Gαi1•GDP at 25 ºC. The left-hand and right-hand plots show the parallel (V) and perpendicular (H) decay curves (black) and IRFs (grey) for the anisotropy decay (35 ps/channel).

Data analysis: The time-resolved anisotropy decay is given by

$$r(t) = \frac{I_{\mathrm{VV}}(t) - I_{\mathrm{VH}}(t)}{I_{\mathrm{VV}}(t) + 2I_{\mathrm{VH}}(t)}$$

The vertical and horizontal decay curves (V and H in Figure S3), obtained with vertical excitation, were fit simultaneously (global fit) by iterative re-convolution of trial decay functions with the IRF using the FluoFit Pro v4.6.6.0 analysis software package (PicoQuant GmbH, Berlin). The anisotropy decay data were fit as sums of exponentials according to the following relationships (2):

$$I_{\mathrm{VV}}(t) = G\frac{1}{3}\sum_{i=1}^{n}\alpha_i e^{-t/\tau_i}\left[1 + 2\sum_{j=1}^{5}\beta_j e^{-t/\phi_j}\right]$$

$$I_{\mathrm{VH}}(t) = \frac{1}{3}\sum_{i=1}^{n}\alpha_i e^{-t/\tau_i}\left[1 - \sum_{j=1}^{5}\beta_j e^{-t/\phi_j}\right]$$

where α_i and τ_i are the amplitude and lifetime of the *i*th intensity decay component; β_j and ϕ_j are the relative amplitude and correlation time of the *j*th rotational decay component, and the sum of

β_j for all anisotropy components is equal to the time-zero limiting anisotropy, r_0. The correction factor $G = \int I_{\mathrm{HV}} dt / \int I_{\mathrm{HH}} dt$ was obtained by using horizontal excitation (i.e., HV and HH) to correct for differences in the efficiencies of the V and H detection channels; under ideal conditions $G = 1$ (28). Goodness of fit was judged by the χ^2 statistic, residuals and their autocorrelation (see below for different decay models). Error estimates of the recovered parameters were calculated at the 95% confidence limit using the support-plane method (3).

Sample preparation: HPLC purified Alexa-labeled Gαi1 complexes were GDP, Ric-8A or GTPγS. 50 mM Tris (pH 8.0), 250 mM NaCl, 2 mM DTT, 0.05% C12E10 and either 100 µM GDP, 1 µM Ric-8A, or 10 µM GTPγS+10 mM Mg^{2+}, for each Gαi1 binding state, respectively were added and used for data acquisition.

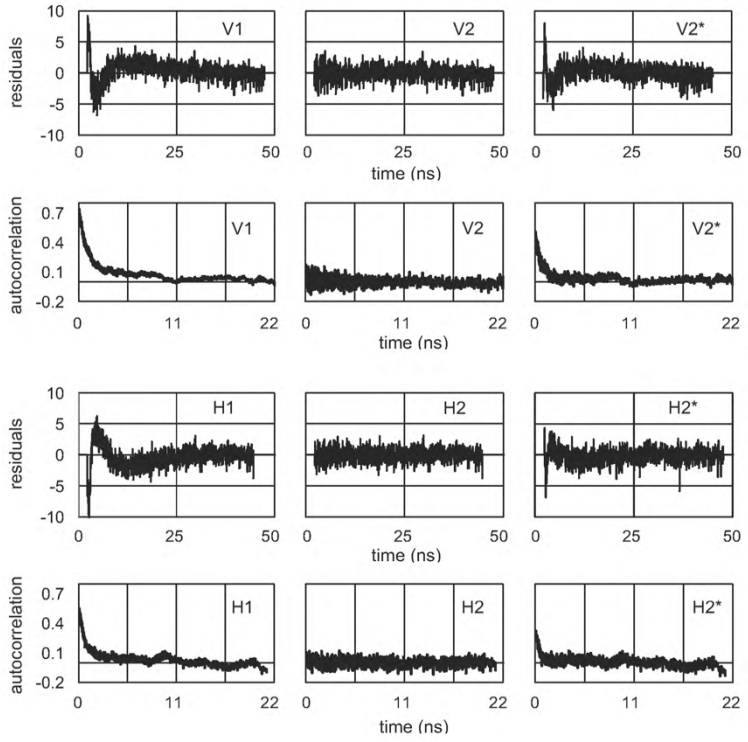

Figure S4 The residuals and their autocorrelation for various fits of the Ax330 Gαi1•GDP anisotropy decay data.

Results for Ax330 Gαi1•GDP: The left-hand column of Figure S4, V1 and H1, shows residuals and autocorrelation of the residuals for fitting the above anisotropy decay data with a single rotational correlation time, which yields a value of 6.59 ns, r_0 of 0.202, and $\chi^2 = 2.91$; the non-randomly distributed residuals and auto-correlation function indicate that a single rotational correlation time model yields a poor fit. Statistically satisfactory fits have χ^2 values close to 1.0; the residuals and autocorrelation function both will be randomly distributed about zero throughout the time range, as in the middle column for V2 and H2, a fit for two unconstrained rotational correlation times. When data for all other complexes were fit with a single rotational correlation time, high χ^2 values and non-random residuals were obtained, indicating that in all cases the Alexa probe is reporting complex dynamics.

The middle column, V2 and H2, shows residuals and their autocorrelation when fitting two unconstrained rotational correlation times. This fit yields short and long correlation times of 0.93 (-0.19, 0.23) ns, $\beta_{short} = 0.127$ (-0.007, 0.007) and 15.31 (-2.15, 3.09) ns, $\beta_{long} = 0.131$ (-0.006, 0.005) with r_0 of 0.258, $\chi^2 = 1.13$. Fixing the long correlation time at 15.05 ns, the average value calculated from FCS data (see below), yields the same parameters and same χ^2 with equivalent residuals and autocorrelation function.

The right-hand column, V2* and H2*, shows residuals and their autocorrelation for two rotational correlation times when the long and short correlation times fixed at 15.05 and 2.31 ns, respectively; the value for the short correlation time was obtained from analysis of the anisotropy decay data of the Ax330 Gαi1:Ric-8A complex with the long correlation time fixed at 53 ns, described below. The sum of β_j gave r_0 of 0.222 and $\chi^2 = 1.73$, indicating that a short correlation time of 2.31 ns does not fit the anisotropy decay data for the GDP complex.

Results for fitting Ax330 Gαi1:Ric-8A data: results for the Ric-8A complex are shown in Figure S5 for three different models, each with two rotational correlation times. The left-hand column, V2 and H2, are the residuals and autocorrelation for an unrestricted analysis. This fit yields a short correlation time of 2.05 (-0.39, 0.48) ns, $\beta_{short} = 0.077$ (-0.008, 0.009), a long correlation time of 47.8 (-7.1, 11.7) ns, $\beta_{long} = 0.225$ (-0.011, 0.008) with r_0 of 0.302, and $\chi^2 = 1.08$. When the long correlation time is fixed at 53 ns, which is the average value for the global rotation of the Ric-8A complexes calculated from FCS data (see below), the short correlation time increases slightly to 2.31 (-0.22, 0.25) ns with $\beta_{short} = 0.082$ (-0.003, 0.003) and $\beta_{long} = 0.219$, yielding a similar r_0 of 0.301, the same χ^2 statistic of 1.08, and similar residuals and autocorrelation.

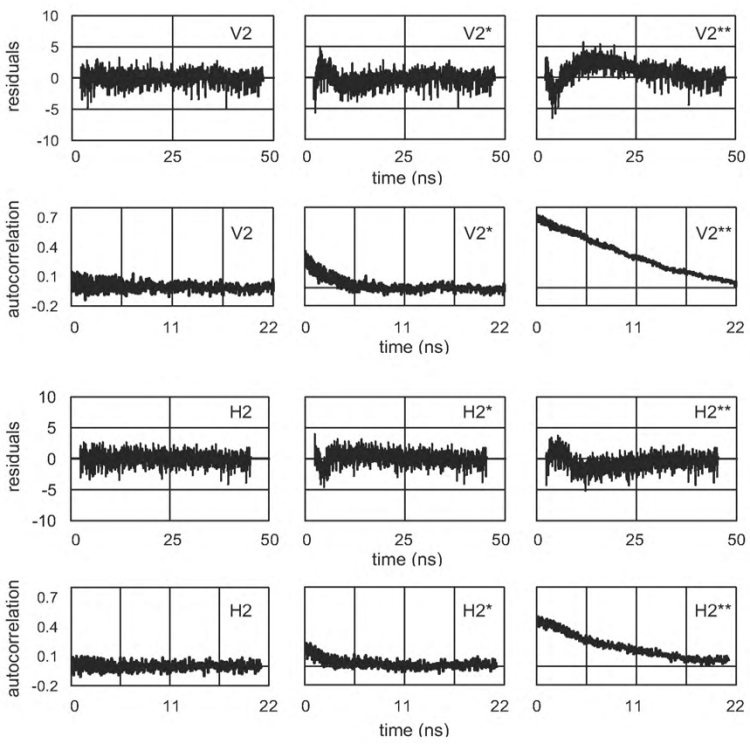

Figure S5 The residuals and their autocorrelation for fits of the Ax330 Gαi1:Ric-8A anisotropy decay data.

The middle column, V2* and H2*, shows residuals and autocorrelation for two rotational correlation times when the shorter component is fixed at 0.93 ns, a value obtained from analysis of the Ax330 Gαi1:Ric-8A complex (above), and the longer component fixed at 53 ns, the value obtained from the FCS data (see below). This gave r_0 of 0.323 and $\chi^2 = 1.37$. The nonrandom residuals and autocorrelation at early times in the decay (within 5 ns) of both V2* and H2* indicate that a short correlation time fixed at 0.93 ns (about half the value of that obtained from either fit described in the preceding analysis) does not fit the anisotropy decay of the Ric-8A complex.

The right-hand column, V2** and H2**, shows residuals and their autocorrelation for two rotational correlation times when the long correlation time is fixed at 15.05 ns, the value obtained from FCS (see below) measurements used in analysis of the Ax330 Gαi1•GDP complex (above).

This gave r_0 of 0.294 with essentially no contribution from a shorter correlation time, and $\chi^2 = 2.60$. Visual inspection of the residuals and their autocorrelation clearly shows that a long rotational correlation time of 15 ns does not fit the anisotropy decay of the Ax330 Gαi1:Ric-8A complex.

FLUORESCENCE CORRELATION SPECTROSCOPY

Data collection: FCS measurements were carried out using an inverted-confocal Olympus IX71 microscope fitted with a 60X 1.2-NA water-objective. A 468-nm pulsed-diode laser (20-60 μW, 20 MHz Model LDH-P-C-470 PicoQuant GmbH, Berlin) was used for excitation. The fluorescence emission was isolated by a 535/50-nm bandpass filter (Chroma Technology Corp., Bellows Falls, VT) with detection using avalanche photodiodes (APD) (Perkin-Elmer model SPCM-AQR-14-FC). The Alexa 488 (C5) β-ME adduct was used to optimize the confocal optical train by measuring the dye's molecular brightness (counts^{-1} molecule^{-1} sec^{-1}), and the confocal volume properties were determined using a translational diffusion coefficient of 420 ± 5 μm^2 s^{-1} at 21.5°C (value and range calculated from the literature (4-6)). Figure S6A shows example data for the Ax330 GDP and Ric-8A complexes and Figure S6B shows residuals from single-species fits. Recovered FCS parameters are listed in Table 1 of the paper.

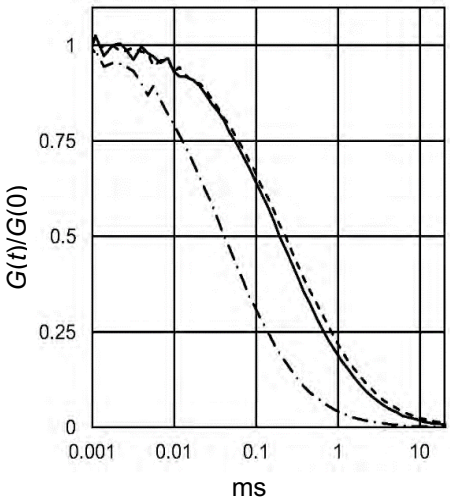

Figure S6A Normalized FCS curves for Ax330 Gαi1:Ric-8A (----), Ax330 Gαi1•GDP (——), and Alexa 488 *β*-ME adduct (-•--•--).

Labeled protein complexes were prepared as described above. One mL of 50-100 pM protein sample was placed in a cylindrical confocal microscope sample chamber fitted with optical grade disposable cover slips.

Typical data collection times were five minutes. SymPhoTime v5.3.2.2 (PicoQuant GmbH, Berlin) software was used for data acquisition and analysis.

Data Analysis: Fluorescence fluctuations in time,

$$\partial F(t) \equiv F(t) - \langle F(t) \rangle,$$

can be induced by a variety of processes and depend on various photo-physical parameters (2). Following the treatment of Schwille *et al.*, (7-10), the normalized fluorescence fluctuation autocorrelation function $G_{ii}(\tau)$, with lag time τ, is defined as:

$$G_{ii}(\tau) = \frac{\langle \partial F_i(t) \cdot \partial F_i(t+\tau) \rangle}{\langle F_i(t) \rangle^2}$$

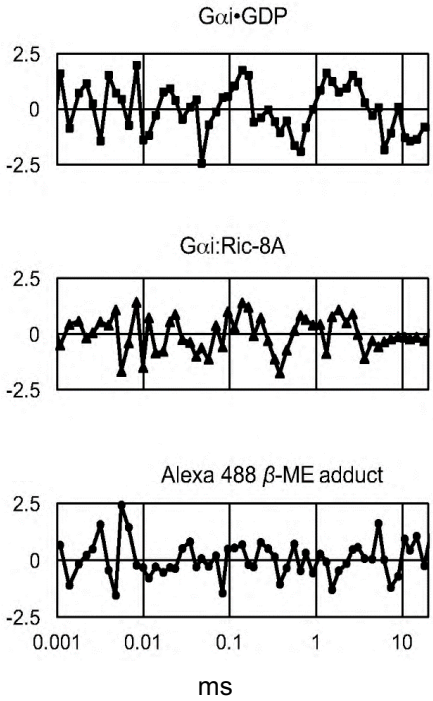

Figure S6 B Residuals for single species fits of Ax330 Gαi1•GDP (Top), Ax330 Gαi1:Ric-8A (Middle), and Alexa 488-*β*-ME adduct (Bottom).

Assuming the intensity fluctuations are due to changes in concentration (so-called number fluctuations), they can be described by a normalized three-dimensional diffusion autocorrelation function for species *i*:

$$G_{ii}(\tau) = \sum_{i=1}^{n} \rho_i (1 + \frac{\tau}{\tau_i})^{-1} (1 + \frac{\tau}{\tau_i \kappa^2})^{-\frac{1}{2}}$$

where $\sum_{i=1}^{n} \rho_i = \frac{1}{\langle N \rangle}$ is the inverse of the average number of molecules inside the effective measurement volume, $V_{eff} = \pi^{\frac{3}{2}} \omega_0^2 z_0$, and $\tau_i = \frac{\omega_0^2}{4D_i}$ is defined as the average lateral diffusion time for a molecule of species *i* through V_{eff}. The ellipticity of V_{eff} is defined as $\kappa = \frac{z_0}{\omega_0}$, the ratio of vertical to horizontal radii. Thus, when V_{eff} is properly calibrated with a known standard, a translational diffusion coefficient (D_i) can be easily derived from the characteristic decay time, τ_i. The shape of $G_{ii}(\tau)$, however, can be significantly distorted by dye converting from the singlet excited state to the triplet state, which is on the same timescale as diffusion and independent of calibration. APD shot-noise and after-pulsing also can contribute to apparent triplet state distortion. Accordingly, a triplet-state "character" τ_T, is incorporated in $G_{ii}(\tau)$:

$$G_{ii}(\tau) = \left(1 - T + Te^{-\frac{\tau}{\tau_T}}\right) \sum_{i=1}^{n} \rho_i (1 + \frac{\tau}{\tau_i})^{-1} (1 + \frac{\tau}{\tau_i \kappa^2})^{-\frac{1}{2}}$$

and $\sum_{i=1}^{n} \rho_i = \frac{1}{\langle N \rangle (1-T)}$.

To reduce shot-noise and effects of after-pulsing, a lifetime gating filter was applied, eliminating the need for cross-correlation (11, 12) . However, a triplet-state correction was still necessary.

Global rotational correlation times, used for fitting anisotropy decay data (above), were calculated by using the Stokes-Einstein and Stokes-Einstein-Debye relations (2, 9):

$$D_{translational} = \frac{k_B T}{6\eta\pi r}$$

and

$$D_{rotational} = \frac{k_B T}{6\eta \left(\frac{4}{3}\pi r^3\right)},$$

respectively, relate translational diffusion to rotational diffusion such that

$$D_{rotational} = D_{translational} \frac{3}{4r^2},$$

where k_B is Boltzmann's constant, T is temperature, η is the viscosity of the medium and r is the hydrodynamic radius of a spherical rotating body.

SUPPORTING REFERENCES

1. Minazzo, A. S., R. C. Darlington and J. B. A. Ross. 2009. Loop dynamics of the extracellular domain of human tissue factor and activation of factor VIIa. Biophys. J. 96, 681-692.

2. Lakowicz, J. R. 2006. Principles of Fluorescence Spectroscopy. Third Edition. New York: Springer Science.

3. Straume, M., S. G. Frasier-Cadoret and M. L. Johnson. 1991. Least-squares analysis of fluorescence data. In: Lakowicz, JR, editor. *Topics in Fluorescence Spectroscopy 2*: Kluwer Academic Publishers. p 177-240.

4. Nitsche, J. M., H. C. Chang, P. A. Weber and B. J. Nicholson. 2004. A transient diffusion model yields unitary gap junctional permeabilities from images of cell-to-cell fluorescent dye transfer between Xenopus oocytes. Biophys. J. 86, 2058-2077.

5. Petrasek, Z. and P. Schwille. 2008. Precise measurement of diffusion coefficients using scanning fluorescence correlation spectroscopy. Biophys. J. 94, 1437-1448.

6. Kapusta, P. 2010. Absolute Diffusion Coefficients:Compilation of References Data for FCS Calibration. Berlin: PicoQuant GmbH.

7. Medina, M. A. and P. Schwille. 2002. Fluorescence correlation spectroscopy for the detection and study of single molecules in biology. BioEssays : news and reviews in molecular, cellular and developmental biology 24, 758-764.

8. Bacia, K. and P. Schwille. 2007. Fluorescence correlation spectroscopy. Methods in molecular biology 398, 73-84.

9. Ries, J. and P. Schwille. 2012. Fluorescence correlation spectroscopy. BioEssays : news and reviews in molecular, cellular and developmental biology 34, 361-368.

10. Bacia, K., E. Haustein and P. Schwille. 2014. Fluorescence correlation spectroscopy: principles and applications. Cold Spring Harbor protocols 2014, 709-725.

11. Bohmer, M., M. Wahl, H. J. Rahn, R. Erdmann and J. Enderlein. 2002. Time-resolved fluorescence correlation spectroscopy. Chem. Phys. Lett. 353, 439-445.

12. Enderlein, J. and I. Gregor. 2005. Using fluorescence lifetime for discriminating detector afterpulsing in fluorescence-correlation spectroscopy. Rev. Sci. Instrum. 76. doi.org/10.1063/1.1863399